

## Application of the differential impedance analysis on the microbiologically induced corrosion of bronze

R. Spotorno\*, G. Ghiara

Department of Chemistry and Industrial Chemistry, University of Genoa, Via Dodecaneso 31, I-16146 Genoa, Italy

Received December 8, 2016    Revised March 6, 2017

In this work, the behavior of a binary Cu-Sn (12wt% Sn) alloy has been studied in presence and absence of bacteria in aqueous solution simulating stagnant fresh water. The corrosion processes have been investigated using the Electrochemical Impedance spectroscopy (EIS) technique. The application of the Differential Impedance Analysis (DIA) allowed identifying three processes attributed to the electrical double layer, electrical properties of the passive film and mass transfer processes at the metal/solution interface. Based on DIA structural analysis, equivalent circuit model was proposed and used for better parametric identification of the impedance data. The formation of a biofilm strongly influenced the passive layer behavior, promoting localized corrosion. Post-experiment characterization performed by Scanning electron microscopy (SEM) supported the electrochemical characterization.

**Key words:** microbiologically induced corrosion, tin-bronze alloys, electrochemical impedance spectroscopy, differential impedance analysis

### INTRODUCTION

Microbiologically Induced Corrosion (MIC) is a phenomenon often considered when non-defined morphologies occur on metallic surfaces. It is linked to microbial activity interacting with the substrate. Bacteria promote the formation of a biofilm which influences the corrosion processes by selective introduction or removal of chemical species at the interface with the metal [1-4].

When MIC occurs an increase of the corrosion potential, associated to biofilm growth, is usually observed. The presence of the biofilm induces local reactions shifting the corrosion potential to a more noble state, therefore increasing the risk of pitting corrosion [4,5]. MIC processes have widely been studied for stainless steel in several environments as a result of interests linked to some applications, focusing on the prevention of failures under operating conditions [6]. Several studies can also be found for copper alloys, when applied as structural or mechanical parts operating in aqueous solutions where they are subject to bacteria colonization [7,8]. Despite the fact that copper is often used as biocide, several types of bacteria are able to become tolerant toward ions and survive in adverse conditions [9,10]. Aerobic bacteria commonly present in fresh water as *Pseudomonas sp.* are known to have a role in copper alloys corrosion [11,12]. They cause the acceleration of the

corrosion processes mainly producing a biofilm capable of creating concentration cells replacing oxygen with CO<sub>2</sub> and acting as chelating agent [12-14]. Among classical electrochemical techniques suitable for the study and evaluation of MIC, electrochemical impedance spectroscopy (EIS) is one of the most powerful tools for monitoring and understanding the corrosion processes. EIS allows obtaining more information related to the system under investigation such as the polarization resistance contributions ( $R_p$ ) that can be used for the calculation of the corrosion rate [1]. The resistive and capacitive contributions related to the processes taking place in the system can also be deconvoluted, however, this operation requires additional and more complicated data analyses. In the classical deconvolution approach, an equivalent circuit model is hypothesized, based on preliminary knowledge of the system under investigation and the recorded spectrum. Then it is parametrically identified by Complex Non-linear Regression Least Squares (CNRLS) fitting procedure [15-18]. Thus the contribution of the model components is evaluated. EIS measurements at different experimental conditions can be additionally acquired in order to evaluate better the influence on the individual contributions and thus to refine the equivalent circuit model. Structural identification is an alternative approach which is very convenient for systems where little or no knowledge is available. This approach consists in the generalized deconvolution of the impedance data using mathematical techniques which do not need *a priori* chosen assumptions.

---

To whom all correspondence should be sent:  
E-mail: roberto.spotorno@edu.unige.it

The Differential Impedance Analysis (DIA) is a technique that applies the structural identification approach [19-22]. It ensures both structural and parametric identification based on the experimental data and thus eliminates the necessity of preliminary working hypothesis. The method applies a local estimator – local operating model (LOM) which is used for the performance of a local parametric analysis by scanning along the analytical coordinate frequency. The LOM describes a simple first order inertial system extended with an additive term [21,22]. The simplest electrical equivalent of its transfer function is a mesh of resistance  $R$  and capacitance  $C$  in parallel, extended with additive term  $Ad$  connected in series, which for electrochemical systems can be additive resistance, most often the resistance of the electrolyte  $R_s$ . The effective time constant  $T = RC$  is also introduced as parameter. The parametric identification of the LOM applies a scanning identification window of one frequency point which makes the use of statistical approach impossible. Thus it is replaced with a deterministic one by extension of the initial set of data (real  $Z'$ , imaginary  $Z''$  components of the impedance and frequency ) with two additional terms – the derivatives of  $Z'$  and  $Z''$  in respect to the frequency. Thus the LOM parameters estimates are determined for every frequency. They form a new experimental set of data (  $\hat{R}_i, \hat{C}_i, \hat{T}_i, \hat{R}_s$  ). The frequency analysis of the LOM parameters estimates  $\hat{P}_{LOM}$  known as Temporal analysis provides for structural and parametric identification. It identifies the number of time constants (steps) involved in the total process, their distribution, and easily defines the rate limiting ones. In the frequency range where the LOM corresponds to the object's behaviour, the temporal plots exhibit plateaux. Their number corresponds to the number of time constants [21,22]. The temporal analysis can qualitatively estimate frequency distribution which is marked as deviation from the plateau-behavior. However, for quantitative analysis, i.e. for structural and parametric identification, a new algorithm, named Secondary DIA, should be used [21, 22]. In this study only DIA is applied. For more precise parametric evaluation CNRLS is performed based on the results obtained by DIA.

The aim of this study is to define the influence of *Pseudomonas sp.* on the corrosion processes of tin-bronzes and their ability to promote localized phenomena applying electrochemical impedance spectroscopy and DIA, supported by post-experimental observations. The experiments were performed on a binary Cu-Sn (12%wt) alloy in

artificial fresh water containing mixed chlorides, nitrates, sulphates and carbonates, in presence and absence of bacteria.

## MATERIALS AND METHODS

A commercial tin-bronze (12 wt % Sn) alloy was chosen for the corrosion experiments in presence and absence of bacteria. Samples were cut from a sheet in pieces of 1 cm x 1 cm x 0.5 cm and additionally treated in order to obtain a suitable microstructure. Recrystallization was promoted by application of a thermo-mechanical treatment combining cold hammering which creates superficial and bulk defects with heating up to 600°C for 12h. Such treatment was performed twice to ensure homogeneity of the solid solution, avoiding the presence of secondary phases. Figure 1 shows the microstructure of the samples prepared for the corrosion testing. They were embedded in epoxy resin leaving an exposed surface of 1 cm<sup>2</sup>. The samples were immersed in the artificial fresh water solution (AFW) with pH 8.1 containing MgSO<sub>4</sub>\*7H<sub>2</sub>O (100 mg L<sup>-1</sup>); MgCl<sub>2</sub>\*6H<sub>2</sub>O (135 mg L<sup>-1</sup>); NaHCO<sub>3</sub> (185 mg L<sup>-1</sup>); Na<sub>2</sub>CO<sub>3</sub> (230 mg L<sup>-1</sup>); KNO<sub>3</sub> (20 mg L<sup>-1</sup>) [21]. The solution conductivity was 1020±80 μS cm<sup>-1</sup>. For tests in the presence of bacteria (BAFW), a *Pseudomonas Fluorescens N3* strain [23, 24] was added to the AFW with a concentration of 1x10<sup>7</sup> CFU mL<sup>-1</sup> (colony forming unit mL<sup>-1</sup>).

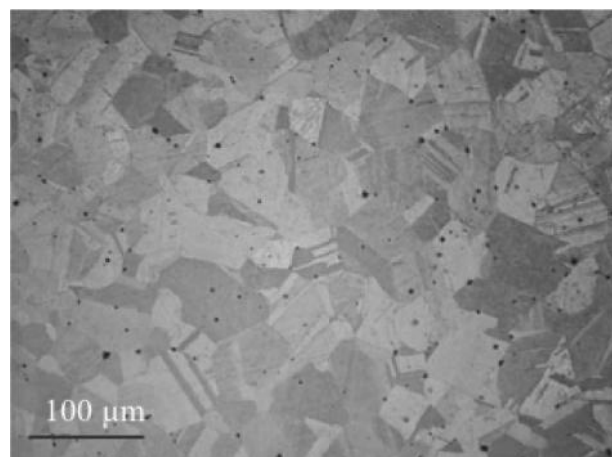


**Fig. 1.** Micrograph of certified material (12 wt% Sn) after thermo-mechanical treatment, 100x, etched with Fe<sub>3</sub>Cl.

The EIS analysis was performed using a three electrode cell with the sample as working electrode (WE), a reference electrode (RE) of Ag/AgCl sat. KCl and a platinum wire as counter electrode (CE) in a volume of 0.3 L in static conditions. The measurements were carried out at the first stabilization of the open circuit potential (OCP) after the immersion of the sample in the solution,

in the frequency range 40kHz-10mHz with an amplitude of the a.c. signal 20mV, using Ivium CompactStat (Ivium Technologies). Structural analysis of the impedance data was carried out applying the DIA technique [21,22]. Based on the DIA, a more precise parametric identification was performed by CNRLS using the software Zview (Schriber Associates Inc.). Post-experiment characterization was carried out by Scanning Electron Microscopy (SEM; Zeiss Evo40, Carl Zeiss, Oberkochen, Germany). Chemical analyses of the surface layers were performed by energy-dispersion x-ray spectroscopy (EDS; Cambridge INCA 300 with PentaFET EDXS detector; Oxford Instruments, Oxfordshire; U.K.) connected to the SEM.

## RESULTS AND DISCUSSION

The recorded impedance spectra are characterized with two arcs (Fig. 2) - a large and incomplete one at low frequencies and a small one at high frequencies. The low frequency arc can be associated to slower processes as mass transfer phenomena which are linked to the dissolution of the metal and the formation of a passive layer on the metal surface [25]. The addition of bacteria to the solution causes a decrease of this arc which indicates increase of the corrosion rate provoked by the microbial activity. The high frequency semicircle corresponds to fast phenomena

which can be attributed to the charge transfer processes [26]. This part of the spectrum is not significantly influenced by the presence of *Pseudomonas* in the solution.

However, a disturbance of the signal at high frequencies limited the measurement, making difficult the identification of its intercept with the real part axis which determines the ohmic resistance.

The performance of the DIA Temporal analysis (Figure 3) shows comparable in shape parametric profiles corresponding to the two impedance spectra. Following the procedure for spectral transformation [20-22], the temporal plots in Fig. 3 are represented in a spectral form (Fig. 4). The intensity of the spectral lines is proportional to the frequency length in which the corresponding parameter's estimate has similar values. Thus every plateau from the Temporal plot is transformed in a spectral peak. The smaller the frequency dispersion, the sharper the spectral maximum.

The temporal plots presented in Fig. 3 can be divided in 3 segments (Fig. 3 - Segments I-III) with different frequency dependence which indicates 3 different steps. The high frequency contribution (segment I) has a plateau-type behavior, thus recognising a process described with a time-constant, which corresponds to the charge transfer. The spectral presentation illustrates in an explicit form the  $R$ ,  $C$  and  $T$  spectral peaks.

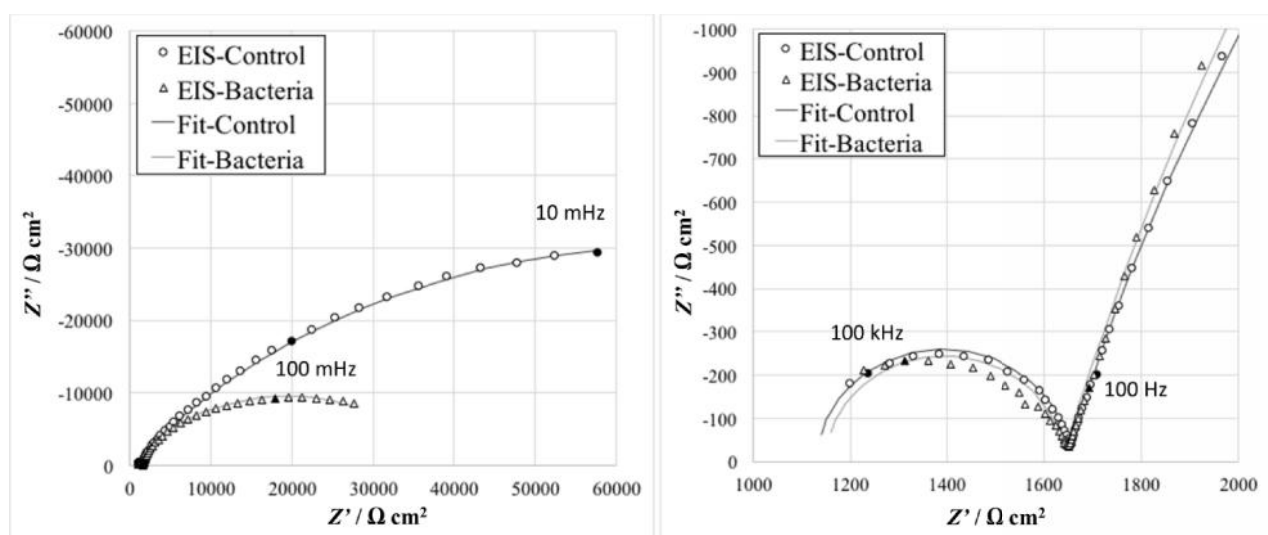


**Fig. 2.** Impedance spectra and fitting results of the two samples in the whole frequency range (left); zoomed high frequency range (right).

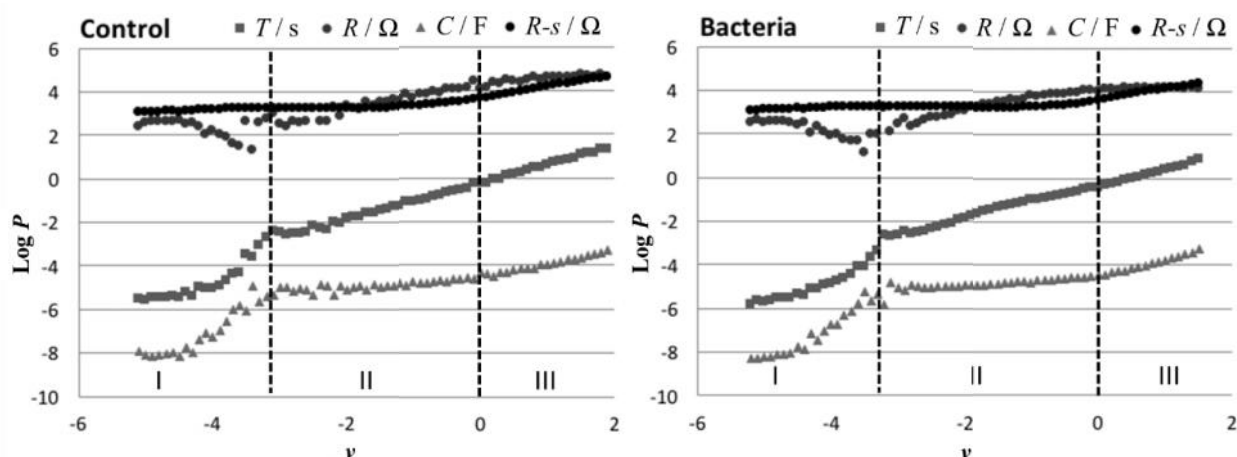


**Fig. 3.** DIA temporal plots of the control sample (left) and the sample with bacteria (right).  $P$  represents the value of the respective effective parameter ( $T, R, C, R_s$ ) and  $\epsilon|| = \lg(\cdot^{-1})$ .

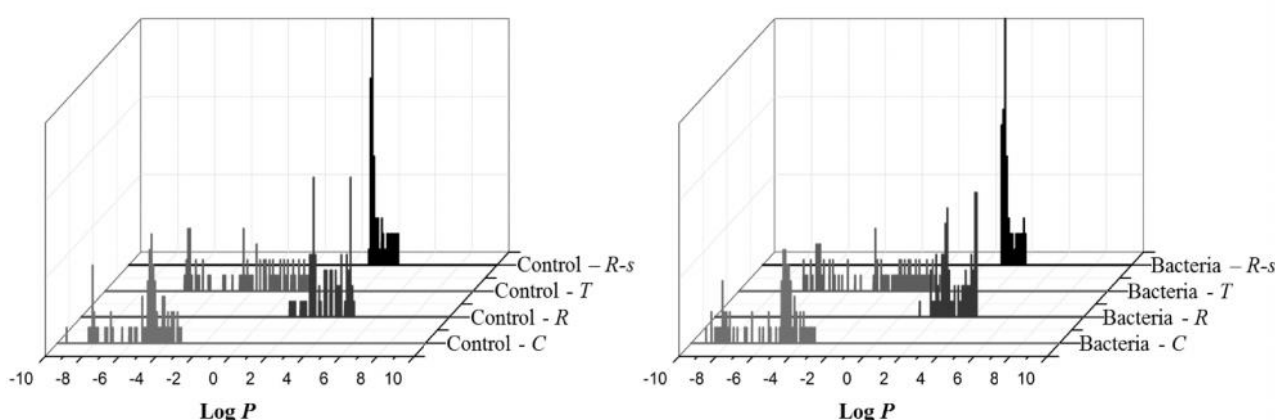


**Fig. 4.** Spectral presentation of the Temporal plots from Fig. 3.

Although the plots are similar for the system with and without bacteria, the presence of bacteria increases the frequency distribution of  $T$ , which is more pronounced for its  $C$  component. At lower frequencies DIA distinguishes two processes (segments II and III) identified by the difference in the frequency dependence of the LOM parameters estimates. For precise structural and parametric identification a Secondary DIA is needed. On this stage those two steps were further modeled with constant phase elements (CPEs) in a proposed equivalent circuit of the system (Fig. 5). The analysis of the  $R$  temporal plot shows that the low frequency step (Segment III) which has the highest level of frequency distribution, is the rate limiting stage, i.e. it gives the biggest contribution in the resistance of the system.

The  $R_s$  spectra allowed identifying the solution resistance of both samples. Even for the bacteria sample, where the first intercept of the real axis was not visible, a peak in the spectral plot was well distinguishable. The solution resistance was estimated to be 1132  $\Omega$  for the control sample and 1150  $\Omega$  when bacteria were present. Such values

are comparable with the results from conductivity measurements of the solution.

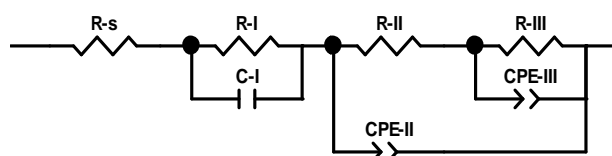


**Fig. 5.** Equivalent circuit used for fitting calculated with measured data.

Although for structural and parametric identification of Segments II and III a procedure of Secondary DIA is needed, the analysis of the corresponding  $R$  and  $C$  spectral peaks pronounced in the Spectral plot gives valuable information. The second  $R$  peak corresponds to segment III and thus it is related to the lowest frequency phenomenon, which was identified as the rate limiting step considering its values, which are one order of magnitude higher than the others. Obviously the resistance of segment II has strongly distributed character and cannot be pronounced on this plot with a spectral maximum. For the capacitance contribution at lower frequencies, a spectral

maximum is pronounced for Segment II. It has more distributed character for the experiment without bacteria.

Based on the structural and parametric information obtained by DIA, an equivalent circuit was proposed (Figure 5) and used for the performance of a fitting procedure on the EIS spectra. The parametric results are summarized in Table I.

**Table I.** CNRLS fitting results.

Sample	Control	Bacteria
Rs /	1132	1150
R-I/	516.8	487.5
C-I (Q)/ F	6.30E-9	4.81E-9
R-II /	6769	15403
CPE-II (Q)/ F	1.92E-5	2.65E-5
CPE-II (n)	0.85	0.84
R-III/	1.31E5	18734
CPE-III (Q)/ F	3.80E-5	1.00E-4
CPE-III (n)	0.49	0.68

The resistance of the solution was identified by the first Rs peak of the DIA spectral analysis. The high-frequency process corresponding to the first semicircle in the EIS spectra was fitted using a resistance in parallel with a capacitor (R-I/C-I), which describes the charge transfer processes at the sample/electrolyte interface. The low-frequency depressed semicircle in Fig. 1 was modelled using a ladder circuit structure with two R//CPE meshes (R-II//CPE-II; R-III//CPE-III) in agreement with the presence of two processes, identified as segments II and III in the temporal plots. Considering the frequency range of the processes and the influence of bacteria, they can be attributed to the electrical properties of the passive film on the sample surface (R-II//CPE-II) and the mass transport at the sample/solution interface (R-III//CPE-III).

Fitting results confirmed the values of the solution resistance calculated by DIA. The high frequency process exhibits lower values for both resistance and capacitance when bacteria are present in the solution. Although the difference in the EIS spectra is small, the correspondent parameters indicate influence of bacteria on the charge transfer phenomena. More significant effect of the bacteria is registered for the processes presented in Segments II and III. The resistance of the second process increases twice (from 6796 to 15403 ) which, related to the electrical properties of the passivation film, signals about the formation of more resistive layer in the presence of

*Pseudomonas*. The increase of the film resistance corresponds to passivation of the sample which could lead to higher risk of pits formation. No significant changes were measured for the associated CPE values. The process which is observed in Segment III was supposed to be related to mass transfer phenomena due to the frequency range and confirmed by the obtained CPE values. In the presence of bacteria the resistance decreased from 1.31E+5 to 18734 indicating higher activity of the localized phenomena. The proposed behavior, associated with the increase of the passivation layer resistance, is consistent with pits formation.

The post-experiment characterization (Figure 6) evidenced the formation of an inner layer constituted by Cu and Sn oxides and areas rich in copper chlorides on the control sample, which is in agreement with other studies on copper alloys in aqueous environment [27].

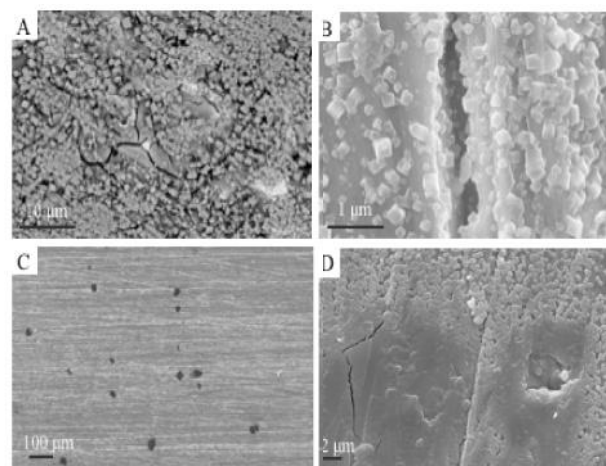


**Fig. 6.** Surface topography of the samples: (a) SEM-BSE 4500x micrograph of a thick passive film of copper and tin oxides and hydroxides under secondary corrosion products identified as CuCl; (b) SEM-SE 15500x micrograph of cracks inside the passive film formed; (c) 100x SEM-SE micrograph of micro-colonies randomly distributed; (d) 4000x SEM-SE micrograph of micro-pits under the removed biofilm.

For samples tested in bacteria rich solution, organic structures were found on the surface. They are formed in the first stage of the biofilm formation (Figure 6c). In several areas, where the biofilm was removed during the sample preparation, localized attacks consisting of micropits were detected (Figure 6d), supporting the electrochemical characterization.

## CONCLUSIONS

The effect of microbiological activity on tin-bronze samples was investigated combining

electrochemical measurements with post-experiment characterization.

The application of a structural approach, based on the DIA technique for EIS data analysis, led to the identification of three corrosion processes for the investigated copper alloy in artificial fresh water. DIA allows studying the distribution of the phenomena in the frequency domain, estimating their resistive and capacitive parameters. It identified the solution resistance despite the disturbance of the signal at high frequencies. The influence of bacteria was visible by changes in the processes distribution using the DIA spectral plots. This information supported the choice of an adequate equivalent circuit to model the corrosion processes for more precise parametric identification. The CNRLS results allowed to estimate quantitatively the changes caused by bacteria in every step of the total process. Minor effects were measured for the charge transfer processes. Microbial activity brought to localized corrosion phenomena. The pit formation, post-experimentally observed, was identified by the decrease of mass transport resistance. For precise structural and parametrical identification of the frequency distributed phenomena which are presented at low frequencies, Secondary DIA will be further applied.

**Acknowledgements:** *The authors would like to thank Prof. Zdravko Stoyanov for sharing his knowledge in electrochemistry and teaching on the Differential Impedance Analysis technique.*

## REFERENCES

1. B. Little, J. Lee, Microbiologically Influenced Corrosion, John Wiley and sons, Hoboken, 2007.
2. P. Cristiani, G Perboni A. Debenedetti, Biocorys 2007 International Conference on Biocorrosion and Materials, Paris, 11–14 June 2007, congress acts, 2007.
3. P. Cristiani, Corrosion monitoring in microbial environments, in L. Yang, Techniques for corrosion monitoring, (2008), Woodhead Publishing, Cambridge, p. 347.
4. W. Characklis, K. Marshall, Biofilms, John Wiley and sons, New York, 1990.
5. P. Marcus (Eds), Corrosion Mechanisms in Theory and Practice, Marcel Dekker, Inc., New York, 2002.
6. P. Cristiani (org.), Biofilm and MIC Monitoring: State of the art, Meeting of Task 5 of Microbiologically Induced Corrosion of Industrial Materials, Venezia, 2000.
7. M. Carvalho, J. Doma, M. Sztylek, I. Beech, P. Cristiani, The study of marine corrosion of copper alloys in chlorinated condenser cooling circuits: The role of microbiological components, *Bioelectrochem.*, **97**, 2 (2014).
8. M. Carvalho, P. Cristiani, Experiences of on-line monitoring of microbial corrosion and antifouling on copper alloys condenser tubes, in M. Malayeri, H. Muller-Steinhagen, A. Watkinson (Eds.) Proceedings of International Conference on Heat Exchangers Fouling and Celaning, Crete Island, Greece, 2011.
9. G. Borkow, J. Gabbay, Copper as a Biocidal tool, Cupron Inc., 2004.
10. S. Kakooei, M. Ismail, B. Ariwahjoedi, Mechanisms of Microbiologically Influenced Corrosion: A Review, *World Appl. Sci. J.*, **17(4)**, 524 (2012).
11. J. Morales, P. Esparza, S. Gonzalez, R. Salvarezza, M. P. Arevalo, The role of *Pseudomonas aeruginosa* on the localized corrosion of 304 stainless steel, *Corros. Sci.*, **34(9)**, 153 (1993).
12. I. Beech, J. Sunner, K. Hiraoka, Microbe–surface interactions in biofouling and biocorrosion processes, *Intern. Microbiol.*, **8**, 157 (2005).
13. J. Busalmen, M. Frontini, S. de Sanchez, Microbial Corrosion: effect of microbial catalase on oxygen reduction, in S. A. Campbell, N. Campbell, F. C. Walsh (eds.), Developments in Marine Corrosion, Royal Society of Chemistry, Cambridge, p. 119(1998).
14. I. Beech, L. Hanjagst, M. Kalaji, A. Neal, V. Zinkevich, Chemical and structural characterization of exopolymers produced by *Pseudomonas* sp. NCIMB 2021 in continuous culture, *Microbiology*, **145**, 1491 (1999).
15. K. Levenberg, A method for the solution of certain non-linear problems in least squares, *Q. Appl. Math.*, **2**, 164 (1944).
16. D. Marquardt, An algorithm for least-squares estimation of nonlinear parameters, *J. Soc. Ind. Appl. Math.*, **11**, 431(1963).
17. B. Boukamp, A nonlinear least squares fit procedure for analysis of immittance data of electrochemical systems, *Solid State Ionics*, **20**, 31 (1986).
18. J. Macdonald, L. Potter, A flexible procedure for analyzing impedance spectroscopy results: Description and illustrations, *Solid State Ionics*, **24**, 61(1987).
19. Z. Stoyanov, Differential impedance analysis - an insight into the experimental data, *Polish J. Chem.*, **71**, 1204 (1997).
20. D. Vladikova, P. Zoltowski, E. Makowska, Z. Stoyanov, Selectivity study of the differential impedance analysis - comparison with the complex non-linear least squares method, *Electrochim. Acta*, **47**, 2943 (2002).
21. Z. Stoyanov, D. Vladikova, “Differential Impedance Analysis“, Marin Drinov Publ. House, Sofia, 2005 (ISBN 954-322-057-3).
22. Z. Stoyanov, D. Vladikova, “Impedance Spectroscopy of Electrochemical Power Sources” in: U. Garcke (Ed.) Encyclopedia of Electrochemical Power Sources, Elsevier, 2009, p. 632 – 642 (ISBN-13: 978-0-444-52093-7; ISBN-10: 0-444-52093-7).
23. JDS 3 I. (2015). Joint Danube Survey 3. A Comprehensive Analysis of Danube Water Quality. Vienna: ICPDR – International Commission for the Protection of the Danube River.

24. G. Sello, S. Bernasconi, F. Orsini, P. Mattavelli, P. Di Gennaro, G. Bestetti, Biocatalyst expressing cis-naphthalene dihydrodiol dehydrogenase from *Pseudomonas fluorescens* N3 catalyzes alcohol and 1,2-diol dehydrogenase reactions, *J. Molecul. Catal. B: Enzymatic*, **52**, 67 (2008).
25. S. Yuan, A. Choong, S. Pehkonen, *Corros. Sci.*, **49**, 4352 (2007).
26. E. Barsoukov, J. Macdonald, *Impedance Spectroscopy: Theory, Experiment, And Applications*, John Wiley And Sons, Hoboken (2005).
27. Cristiani, G. Rocchini, F. Mazza, *Microbial Corrosion Proc. 3th International Efc Workshop Portugal 1994*, (Estoril) 13-16 March 1994 Ed. A.K. Tiller And C.A.C Sequeira, Estoril, The Institute Of Materials, P. 243 - 260, 1995.

( )

8 2016 ; 6 2017 .

( )

Cu-Sn (12wt% Sn)

( )

(SEM).